



OPEN

Computational framework of cobalt ferrite and silver-based hybrid nanofluid over a rotating disk and cone: a comparative study

Umar Farooq¹, Hassan Waqas², Nahid Fatima³, Muhammad Imran¹, Sobia Noreen⁴, Abdul Bariq⁵✉, Ali Akgül^{6,7,8} & Ahmed M. Galal^{9,10}

The dominant characteristics of hybrid nanofluids, including rapid heat transfer rates, superior electrical and thermal conductivity, and low cost, have effectively piqued the interest of global researchers. The current study will look at the impacts of a silver and cobalt ferrite-based hybrid nanofluid with MHD between a revolving disk and cone. The collection of partial differentiable equations is converted into a set of ODEs via similarity transformations. We used the Homotopy analysis approach from the BVP4c 2.0 package to solve the ordinary differential equations. The volume proportion of nanoparticles increases and the temperature distribution profile also increased. It is more efficient for metallurgical, medicinal, and electrical applications. Furthermore, the antibacterial capabilities of silver nanoparticles might be used to restrict the growth of bacteria. A circulating disc with a stationary cone has been identified to provide the optimal cooling of the cone disc device while maintaining the outer edge temperature constant. This study's findings might be useful in materials science and engineering. The usage of hybrid nanofluid in heat transfer and heat pumps, coolants in manufacturing and production, producing cooling, refrigerators, solar thermal collectors, and heating, air conditioning, and climate control applications are only a few examples.

Important expansion has been developed in the variety of science and the vast range of demands for practical nanotechnology in current decades. Nanoparticles have a wide range of possible uses, like biomedical, biotechnology, crystal chemistry, statistical modeling, and disciplines such as sociology, petroleum neuroscience, and so on. Surface textures, shapes, and proportions are some of the additional physical properties of nanoparticles that must be measured for an accurate representation. Nanoparticles are used in a broad range of interdisciplinary fields such as pharmaceutical products, thermal devices, servers, nuclear reactors, chemical plants, and so on. CNTs can also be used in paint, polymer, and indirect interaction with a mucous membrane. In general, nanomaterials technologies focus on increasing the proficiency, durability, and swiftness of existing processes. Nanofluids are legislature fluids made up of micrometers particles. They have special physical properties and engineered carbon nanotubes that can be used in several fields, namely chemical processes, safety, environmental, chemistry, and manufacturing, due to their semi-nanoscale size. Within the definition, nanomaterials must specifically be classified as such within a range of 1–100 nm under one of their consistency ranges, although their other measurements fall outside of that range. Choi¹ was recognized as the first to discuss the idea of nanofluids. Buongiorno² identified thermophoresis results and Brownian motion as critical factors that influence the capability of materials production to transmit temperature. Katiyar et al.³ examined the basic dynamic

¹Department of Mathematics, Government College University, Faisalabad 38000, Pakistan. ²School of Energy and Power Engineering, Jiangsu University, Zhenjiang 2122013, China. ³Department of Mathematics and Sciences, Prince Sultan University, Riyadh 11586, Saudi Arabia. ⁴Department of Chemistry, Government College Women University, Faisalabad 38000, Pakistan. ⁵Department of Mathematics, Laghman University, Mehtarlam 2701, Laghman, Afghanistan. ⁶Department of Computer Science and Mathematics, Lebanese American University, Beirut, Lebanon. ⁷Department of Mathematics, Art and Science Faculty, Siirt University, 56100 Siirt, Turkey. ⁸Department of Mathematics, Mathematics Research Center, Near East University, Near East Boulevard, 99138 Nicosia/Mersin 10, Turkey. ⁹Department of Mechanical Engineering, College of Engineering in WadiAlddawasir, Prince Sattam Bin Abdulaziz University, Al-Kharj, Saudi Arabia. ¹⁰Production Engineering and Mechanical Design Department, Faculty of Engineering, Mansoura University, Mansoura P.O 35516, Egypt. ✉email: abdulbariq.maths@gmail.com

effectiveness technique for fluid motion in porous media. In a virtual sample with a temperature gradient, Hayat et al.⁴ examined the stream of fluid (Carreau fluid). Tilili et al.⁵ expressed the flow of Maxwell nanofluid in the reality of heat distribution and generative influences. Maxwell fluid flow through vertical surfaces with thermal flux open heat transfer was studied by Shah et al.⁶. The expanded cylinder was used by Sohail et al.⁷ to understand the measure of Sutterby fluid. The Darcy-Forchheimer heat property of MHD hybrid nanomaterials flow due to strained cylinders was investigated by Saeed et al.⁸. Babazadeh et al.⁹ developed a hypothetical model for nanomaterials migration on the inside of a porous vacuum. Ullah et al.¹⁰ simulated the heat exchange in a copper-oxidized water-based circular cylinder that was partially heated. The consequences of nanofluid on motile bacteria and Wu's slip were explored by Li et al.¹¹. Waqas et al.¹² investigated the influence of melting on nanofluid flow through a stretched cylinder. Rashid et al.¹³ computed the magnetic flux-related mobility of nanofluids based on adsorption. Xian et al.¹⁴ discovered a steady nanofluid developed by displacing titanium dioxide (TiO₂) and cellulose nanocrystals in a two-step process of purified water. Rabbi et al.¹⁵ examined the physical fields of convective heat in a steel column of Cu-H₂O non-material for various thermostat-sink combinations using the convolution neural network technique as an operative predictive method. Ghalambaz et al.¹⁶ studied the results of conjugate energy transfer in a horizontal pipe of a novel nanofluid flow (Ag-MgO/water hybrid nanofluid). Humnic and Humnic¹⁷ investigated the features of nanofluid and hybrid nanofluid processing in different thermal methods for different boundary climates and health conditions. Tayebi¹⁸ examined the impact of entropy production caused by natural temperature distribution in a tunnel leading between parallel fluorescence microscopy exercise bike cylinders. The effect of different detergents and ultraviolet times on the stabilization and biomedical applications of hybrid supernatant was measured by Xian et al.¹⁹. Awais et al.²⁰ studied the influence of Magnetohydrodynamics on flow adhesives using mechanical and tribological hybrid nanofluid. Waini et al.²¹ explored the MHD convective flow and temperature change of a hybrid nanofluid passing over a porous stretching wedge. Farooq et al.²² evaluated the impact of Carreau nanofluid bioconvection flow using modified Cattaneo-Christov expressions. Reddy et al.²³ examined the consequence of nanofluid flow via square cavity using entropy generation and heat transfer measurements. Reddy et al.²⁴ studied the heat transmission effects of a hybrid nanofluid flow from inside a container. Sreedevi and Reddy²⁵ evaluated the effects of heat transmission and entropy production analyses on a hybrid nanofluid within a cavity. Sudarsana and Sreedevi²⁶ explored the impact of heat transfer analyses on the nanofluid within a cylinder. Sreedevi and Reddy²⁵ investigated the thermal transmission and entropy formation of a nanofluid via a cavity. Reddy et al.²⁷ studied the impact of MHD flow heat and mass transportation features of a nanofluid via a cone. Reddy et al.²⁸ inspected the impact of hybrid nanofluid characteristics on a slip-affecting sheet. Dero et al.²⁹ investigated hybrid nanofluids' impact on suction/injection applications. Haq et al.³⁰ explored the surface effects of a radiative viscous hybrid nanofluid based on theoretical research. The effects of curved radiated surfaces on a modified hybrid nanofluid model were examined by Abbasi et al.³¹. Hassan et al.³² looked at how heat and mass transfer with hybrid nanofluids. The consequences of hybrid nanofluid flow on a curved stretched sheet were investigated by Madhukesh et al.³³. Reddy and Sreedevi³⁴ studied the influence of heat and mass transmission as well as entropy formation in a hybrid nanofluid. More work on nanofluid and hybrid nanofluid are carried out^{12,35-40}.

Current research work aims to analyze the comparative investigation of Cobalt ferrite (COFe₂O₄) nanofluid and Silver (Ag), Cobalt ferrite (COFe₂O₄) hybrid nanofluid flow over a disk and cone. In this study, we looked at the three-dimensional flow of hybrid nanofluid and nanofluid. It has been demonstrated that hybrid nanofluids greatly increase the thermal efficiency of basic fluids when contrasted to other fluids. The nonlinear problem was evaluated using the Homotopy analysis approach, methodology, and BVPh 2.0 software, and this method was compared to the numerical (ND-solve) method. We used the computational tool MATHEMATICA to compute the graphical flow patron of the flow parameter. Silver nanoparticles are used to modulate a variety of actions, including antibacterial, antifouling, chemotherapeutic, antiviral, and drug-delivery systems. This research work will be an excellent improvement on the existing research on the flow of nanofluids across cone and disk. Silver nanoparticles are increasingly being used in a range of industries due to their unique physical and chemical properties, including medicine, food, socialized medicine, consumer electronics, and industrial. Among them include optical, electrical, and thermal properties, as well as high electrical conductivity and biological properties. Because of its features, cobalt ferrites have been widely used in sensors, recording devices, magnetic cards, solar panels, magnetic medication delivery, pharmaceuticals, catalysis, and biotechnology.

Physical description and modeling

Here is the incompressible flow of hybrid nanoparticles and based fluid over both the geometry disk and cone. Here (r, ϕ, z) are the cylindrical coordinate of the cone & disk and (B_0) magnetic field assistance in the direction z , the induced magnetic field is neglected. Here the hybrid nanoparticles Ag + COFe₂O₄ and COFe₂O₄ based fluid is used. The angular velocities of the pipe and disk are denoted $(\omega \& \Omega)$ individually. Figure 1 depicts the flow process.

The main equations are^{41,42}:

$$u_r + w_z + \frac{u}{r} = 0 \quad (1)$$

$$\rho_{hmf} \left[uu_r + ww_z - \frac{v^2}{r} \right] = -p_r + \mu_{hmf} \left[u_{rr} + u_{zz} + \frac{1}{r} u_r - \frac{v}{r^2} \right] - \sigma_{hmf} B_0^2 u, \quad (2)$$

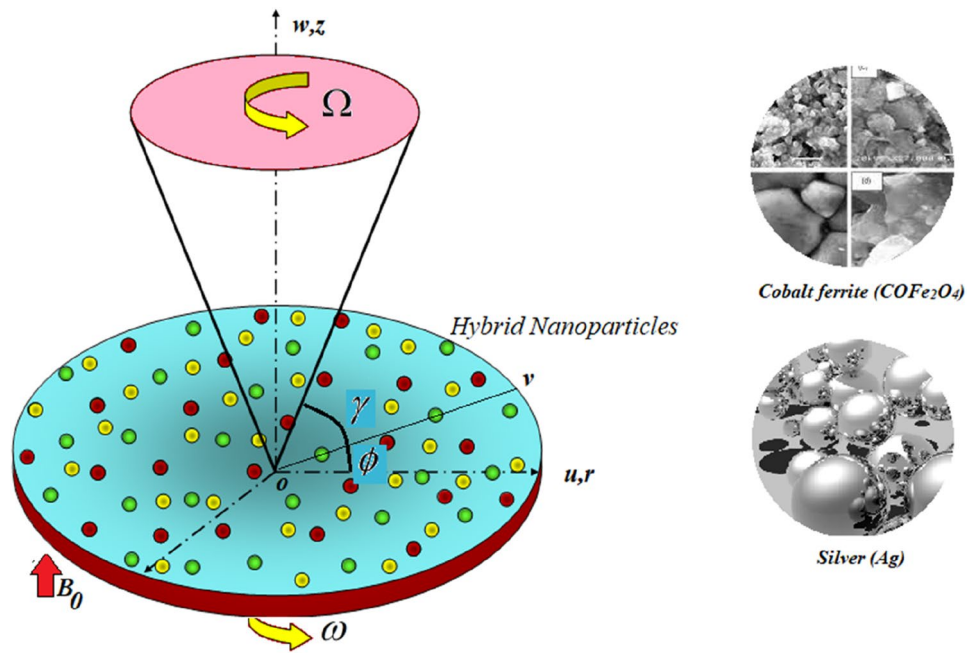


Figure 1. Flow geometry of the problem.

$$\rho_{hnf} \left[uv_r + wv_z - \frac{uv}{r} \right] = \mu_{hnf} \left[v_{rr} + v_{zz} + \frac{1}{r} v_r - \frac{v}{r^2} \right] - \sigma_{hnf} B_0^2 v, \tag{3}$$

$$\rho_{hnf} [uw_r + ww_z] = -p_z + \mu_{hnf} \left[w_{rr} + w_{zz} + \frac{1}{r} w_r \right], \tag{4}$$

$$(\rho c_p)_{hnf} [uT_r + wT_z] = k_{hnf} T_{zz} + \sigma_{hnf} B_0^2 (u^2 + v^2), \tag{5}$$

where (u, v, w) components of speed, While (σ_{hnf}) is the electrical conduction, (B_0) is the magnetic strength, $((\rho c_p)_{hnf})$ heat capacitance, (p) the pressure of the fluid, (μ_{hnf}) dynamic viscosity, (ρ_{hnf}) density, and (k_{hnf}) thermal conductivity respectively.

Boundary conditions^{41,42}:

$$\left. \begin{aligned} & [u(=0)], \quad [w(=0)], \quad [T(=T_w)], \quad [v(=\omega r)], \\ & [z(=0)] \\ & (u(=0)), \quad [w(=0)], \quad [T(=T_\infty)], \quad [v(=\Omega r)], \\ & [z(=r \tan \gamma)], \end{aligned} \right\} \tag{6}$$

Here γ show the angle between the disk and the cone.

Similarity transformations^{41,42}:

$$\left. \begin{aligned} [U_w f(\zeta)] = u = \left[\frac{v_f f(\zeta)}{r} \right], v = \left[\frac{g(\zeta) v_f}{r} \right] = [U_w g(\zeta)], \zeta = \left[\frac{z}{r} \right], \\ w = \left[\frac{v_f h(\zeta)}{r} \right] = [U_w h(\zeta)], p = \left[\frac{\rho v_f^2 P}{r^2} U_w^2 \rho \cdot p \right], \theta = \left[\frac{T - T_\infty}{T_w - T_\infty} \right] \end{aligned} \right\} \tag{7}$$

Here $M = \left(\frac{v_f \sigma_f B_0^2}{\rho_f U_w^2} \right)$ the magnetic parameter, (U_w) is the surface velocity, and $Pr = \left(\frac{\mu_f C_p}{k_f} \right)$ the Prandtl number.

Now, by using (7) the model of Eq. (2–6) is as:

$$h' - \zeta f' \} = 0, \tag{8}$$

$$\left. \begin{aligned} &3\zeta f' + (1 + \zeta^2)f'' + (1 - \phi_{CoFe_2O_4})^{2.5}(1 - \phi_{Ag})^{2.5} \\ &\times [\zeta f f' - h f' + f^2 - g^2] \\ &\left[(1 - \phi_{Ag}) \left(1 - \left(1 - \frac{\rho_{CoFe_2O_4}}{\rho_f} \right) \phi_{CoFe_2O_4} \right) + \phi_{Ag} \left(\frac{\rho_{Ag}}{\rho_f} \right) \right] \\ &+ (1 - \phi_{CoFe_2O_4})^{2.5}(1 - \phi_{Ag})^{2.5}[2p - MF + \zeta p'] \end{aligned} \right\} = 0, \tag{9}$$

$$\left. \begin{aligned} &g''(1 + \zeta^2) + g'3\zeta - (1 - \phi_{CoFe_2O_4})^{2.5}(1 - \phi_{Ag})^{2.5}[\zeta f g' - h g'] \\ &\left[(1 - \phi_{Ag}) \left(1 - \left(1 - \frac{\rho_{CoFe_2O_4}}{\rho_f} \right) \phi_{CoFe_2O_4} \right) + \phi_{Ag} \left(\frac{\rho_{Ag}}{\rho_f} \right) \right] - (1 - \phi_{CoFe_2O_4})^{2.5}Mg(1 - \phi_{Ag})^{2.5} = 0 \end{aligned} \right\}, \tag{10}$$

$$\left. \begin{aligned} &(1 + \zeta^2)h'' + 3\zeta h' + (1 - \phi_{CoFe_2O_4})^{2.5}(1 - \phi_{Ag})^{2.5} \times [d] [-hh' + h + \zeta fh' + fh] \\ &-(1 - \phi_{CoFe_2O_4})^{2.5}(1 - \phi_{Ag})^{2.5}p' = 0 \end{aligned} \right\}, \tag{11}$$

$$\left. \begin{aligned} &\frac{k_{hmf}}{k_{nf}} [\zeta(1 - 2n)\theta' + n^2\theta + (1 + \zeta^2)\theta''] + [\zeta f \theta' - n f \theta - h \theta'] \\ &Pr \left[(1 - \phi_{Ag}) \left(1 - \left(1 - \frac{(\rho C_p)_{CoFe_2O_4}}{(C_p \rho)_f} \phi_{CoFe_2O_4} \right) + \frac{(\rho C_p)_{Ag} \phi_{Ag}}{(C_p \rho)_f} \phi_{Ag} \right) \right] \\ &+ \frac{M}{(1 - \phi_{Ag})^{2.5}(1 - \phi_{CoFe_2O_4})^{2.5}}(f^2 + g^2) = 0 \end{aligned} \right\}, \tag{12}$$

Boundary conditions:

$$\left. \begin{aligned} &f(0)(= 0), \quad \theta(0)(= 1), \quad h(0)(= 0), \\ &g(0)(= Re_\omega), \quad g(\zeta_0)(= Re_\Omega), \\ &f(\zeta_0)(= 0), \quad (\zeta_0)(= 0), \quad h(\zeta_0)(= 0) \end{aligned} \right\}, \tag{13}$$

The volume fraction of nanoparticles is $\phi_{CoFe_2O_4}$ and ϕ_{Ag} . Here (σ_{hmf}) is electrical conduction, (ρ_{hmf}) density, (ν_{hmf}) kinematic viscosity, (k_{hmf}) thermal conductivity, and $(C_{p,hmf})$ certain heat.

$$\left. \begin{aligned} &Nu_d = -\frac{k_{hmf}}{k_{nf}}\theta'(0), \\ &Nu_c = -\frac{k_{hmf}}{k_{nf}}\theta'(\zeta_0) \end{aligned} \right\}. \tag{14}$$

Here Nu_c is the Nusselt number for the cone and Nu_d the disk.

Numerical procedure

In this article, we have used HAM to solve the modeled equations. Liao’s HAM approach solves all high solutions by a sufficient choice of model parameters to enable a divergent sequence solution. In mathematical approaches, HAM can solve boundary value problems. In contrast to perturbation systems, HAM solutions do not require the collection of small/large parameters. Rather than the physical quantity, the auxiliary parameter controls the convergence of the sequence solutions. HAM also gives us the freedom to use our first-guess calculations while having the flow system. The amount of residual error is estimated using the BVP 2.0 to show the convergence speed. This approach selects preliminary estimations that the boundary conditions. To run the MATHEMATICA tool using the HAM technique, initial guesses are needed.

$$\left. \begin{aligned} &f_0(\zeta)(= 0), \quad g_0(\zeta) \left(= \frac{(Re_\Omega - Re_\omega)}{\zeta_0} \zeta + Re_w \right), \\ &h_0(\zeta)(= 0), \quad \theta_0(\zeta) \left(= \frac{\zeta_0 - \zeta}{\zeta_0} \right) \end{aligned} \right\}, \tag{15}$$

So,

$$\ell_h(h) = h'', \ell_\theta(\theta) = \theta'', \ell_f(f) = f'', \ell_g(g) = g'' \tag{16}$$

The expanded form

$$\ell_f[\chi_1 + \chi_2 \zeta] = 0, \ell_g[\chi_3 + \chi_4 \zeta] = 0, \ell_h[\chi_5 + \chi_6 \zeta] = 0, \ell_\theta[\chi_7 + \chi_8 \zeta] = 0. \tag{17}$$

From Eqs. (09–12) as

$$\varepsilon_m^f = \left(\frac{1}{n+1} \right) \sum_{x=1}^n \left[N_f \left(\left(\sum_{y=1}^m f(\zeta) \right), \left(\sum_{y=1}^m g(\zeta) \right), \left(\sum_{y=1}^m h(\zeta) \right) \right)_{\zeta=x\delta\zeta} \right]^2, \tag{18}$$

$$\varepsilon_m^g = \left(\frac{1}{n+1} \right) \sum_{x=1}^n \left[N_g \left(\left(\sum_{y=1}^m h(\zeta) \right), \left(\sum_{y=1}^m f(\zeta) \right), \left(\sum_{y=1}^m g(\zeta) \right) \right)_{\zeta=x\delta\zeta} \right]^2, \tag{19}$$

$$\varepsilon_m^h = \left(\frac{1}{n+1} \right) \sum_{x=1}^n \left[N_f \left(\sum_{y=1}^m h(\zeta) \right)_{\zeta=x\delta\zeta} \right]^2, \tag{20}$$

$$\varepsilon_m^\theta = \left(\frac{1}{n+1} \right) \sum_{x=1}^n \left[N_\theta \left(\left(\sum_{y=1}^m f(\zeta) \right), \left(\sum_{y=1}^m \theta(\zeta) \right), \left(\sum_{y=1}^m g(\zeta) \right) \right)_{\zeta=x\delta\zeta} \right]^2, \tag{21}$$

$$\varepsilon_m^t = \varepsilon_m^f + \varepsilon_m^g + \varepsilon_m^h + \varepsilon_m^\theta. \tag{22}$$

Results and discussion

The system (09–12) is numerically solved by the Homotopy analysis technique. Noticeable performances of the interesting constraints on velocity and temperature are graphically investigated. By taking nonlinear flow parameters of nanofluid and hybrid nanofluid flow traveling through a rotating disk and cone are addressed. To solve the model’s non-linear boundary value problem, the ND-solve approach in the MATHEMATICA tool using the HAM technique is employed. This method is used to address the boundary value issue of an ordinary differential comparison. This section’s main goal is to define and expound on the dimensionless parametric impact on flow velocity and temperature. To test the accuracy of the suggested model, we repeated the method with a wide range of parameter values. The values of these parameters have a significant impact on the convergence of these series. The performance of the volume amended of nanoparticles (ϕ_1) on the velocity distribution profile $F(\zeta)$ is noticed in Fig. 2. It can be understood that the velocity distribution profile $F(\zeta)$ has declining performance for distension estimates of the capacity portion of nanoparticles (ϕ_1). Here are trampled lines for hybrid nanofluid $Ag + COFe_2O_4$ and dash lines for nanofluid $COFe_2O_4$. Figure 3 designates the demonstration of the density segment of nanoparticles (ϕ_2) against the velocity distribution profile $F(\zeta)$. The velocity profile $F(\zeta)$ is condensed by the advanced extent of the volume fraction of nanoparticles (ϕ_2). The inspiration for the velocity distribution profile $F(\zeta)$ in terms of the magnetic parameter (M) is indicated in Fig. 4. The boosting variation of the magnetic parameter (M) falls in the velocity distribution profile $F(\zeta)$. This is owing to the magnetic force that affected the fluid motion, a resistant force is produced which hampers the movement of the fluid. Here are solid lines for hybrid nanofluid $Ag + COFe_2O_4$ and dashes lines for nanofluid $COFe_2O_4$. The performance of the magnetic parameter (M) over the velocity distribution profile $G(\zeta)$ of fluid is detected in Fig. 5. From the figure, it can be seen that the swiftness distribution profile $G(\zeta)$ has decreasing behavior for the higher magnetic parameter (M).

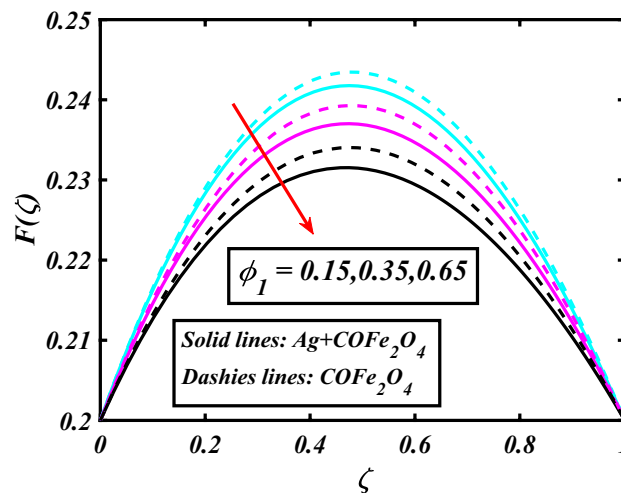


Figure 2. Demonstration of ϕ_1 through $F(\zeta)$.

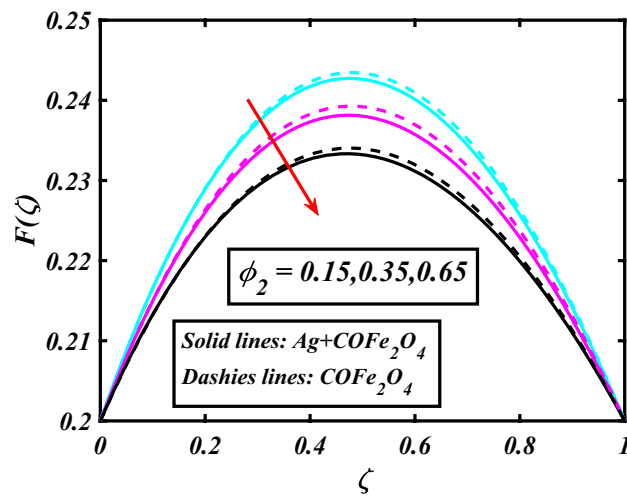


Figure 3. Demonstration of ϕ_2 through $F(\zeta)$.

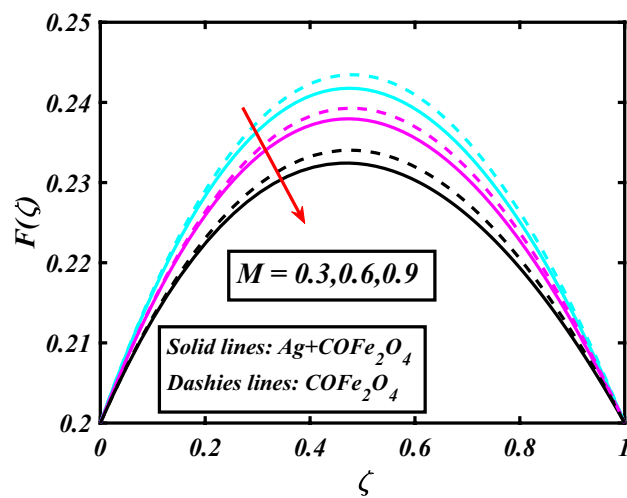


Figure 4. Demonstration of M through $F(\zeta)$.

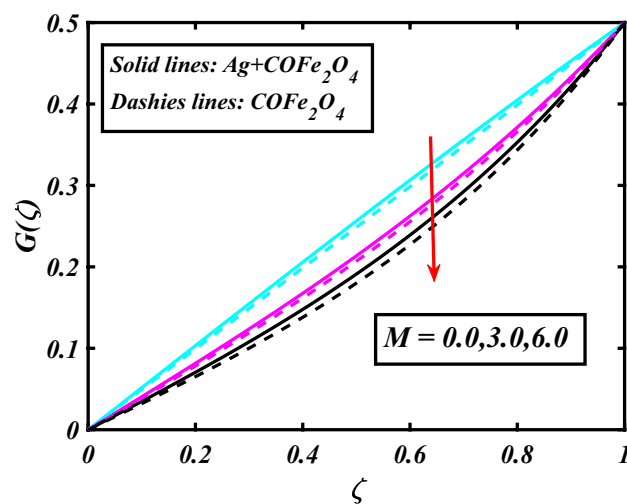


Figure 5. Demonstration of M through $G(\zeta)$.

A magnetic field is a vector field that explains the magnetic impact on electric currents, current flow, and magnetic fluids. A flowing charge in a magnetic field is subjected to a force that is perpendicular to both its velocity and the magnetic field. Figure 6 defines the presentation of the volume segment of nanoparticles (ϕ_1) versus the momentum distribution profile $G(\zeta)$. The velocity distribution profile $G(\zeta)$ is reduced by the increased intensity of the volume segment of nanoparticles (ϕ_1). Here are compacted lines for hybrid nanofluid $Ag + COFe_2O_4$ and dash outlines for nanofluid $COFe_2O_4$. Figure 7 illustrates the power concentration of nanoparticles (m) on the velocity distribution profile $G(\zeta)$. The cumulative principles of concentration of nanoparticles (m) increased the swiftness distribution profile $G(\zeta)$. The concentration of nanoparticles (m) is directly associated with the velocity of the fluid. Here are solid lines for hybrid nanofluid $Ag + COFe_2O_4$ and dashes lines for nanofluid $COFe_2O_4$. The salient features of the volume segment of nanoparticles (ϕ_2) on the high-temperature distribution profile $\theta(\zeta)$ are deliberated in Fig. 8. The lines of graphs display that the rising reliabilities of the volume segment of nanoparticles (ϕ_2) increased the temperature distribution profile $\theta(\zeta)$. The features of the volume segment of nanoparticles (ϕ_1) via the temperature dispersal profile $\theta(\zeta)$ are pictured in Fig. 9. The temperature dissemination profile $\theta(\zeta)$ is enhanced by the intensifying ethics of the volume segment of nanoparticles (ϕ_1). Here comparative study is investigated and solid lines for hybrid nanofluid $Ag + COFe_2O_4$ and dashes lines for nanofluid $COFe_2O_4$.

Table 1 shows the thermophysical properties of nanofluid. Table 2 analyzed the thermophysical properties of a hybrid nanofluid. Table 3 shows the importance of the thermophysical properties of nanoparticles including such (Ag) and ($COFe_2O_4$) with base fluid Water. Table 4 displayed the shape factor of particles like a sphere, hexahedrons, tetrahedrons, cylinders, columns, and lamina. Table 5 shows the variation of magnetic parameters via the Nusselt number. It shows good agreement between published and current work. Table 6 analyzed the

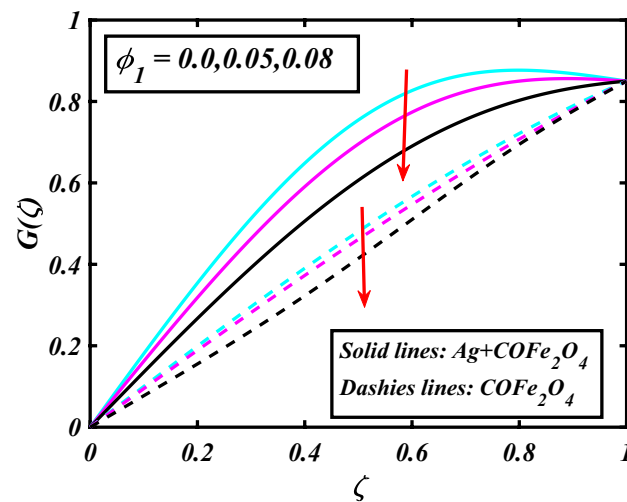


Figure 6. Demonstration of ϕ_1 through $G(\zeta)$.

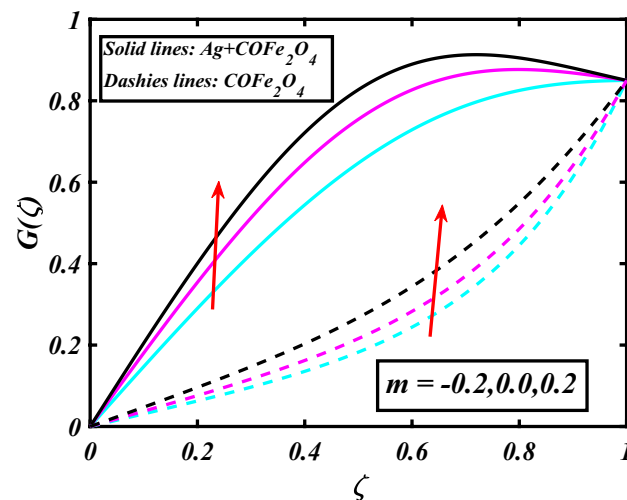


Figure 7. Demonstration of m through $G(\zeta)$.

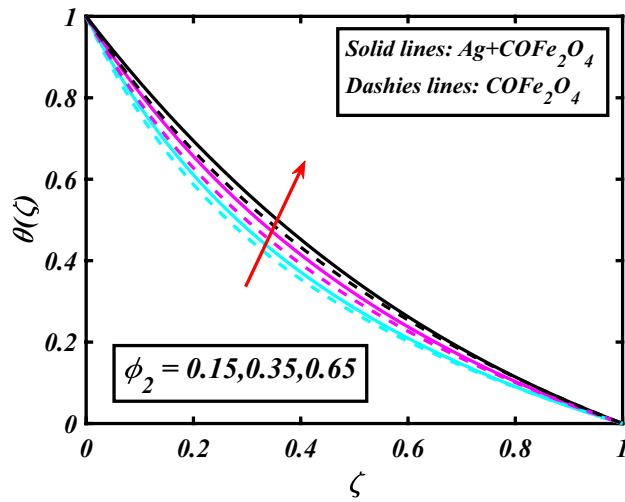


Figure 8. Demonstration of ϕ_2 through $\theta(\zeta)$.

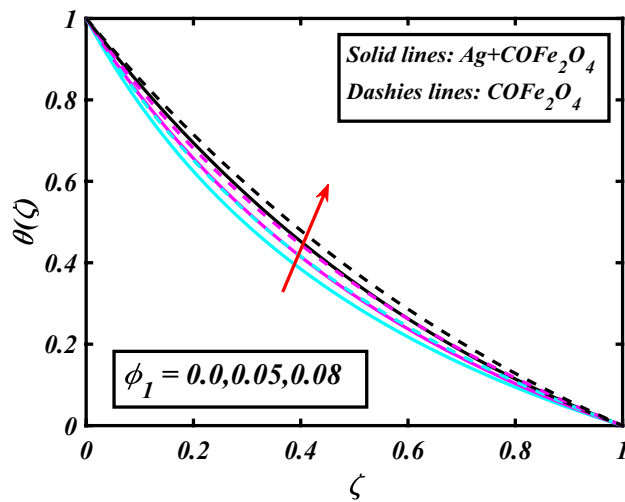


Figure 9. Demonstration of ϕ_1 through $\theta(\zeta)$.

Properties	Formula
Density (ρ_{nf})	$\rho_{nf} = \phi_1(\rho_{s1}) + \rho_f(1 - \phi_1)$
Viscosity (μ_{nf})	$\mu_{nf} = \mu_f / (1 - \phi_1)^{2.5}$
Heat capacity ($\rho C_p)_{nf}$)	$(\rho C_p)_{nf} = \phi_1(\rho C_p)_{s1} + (\rho C_p)_f(1 - \phi_1)$
Thermal conductivity (k_{nf})	$\frac{k_{nf}}{k_f} = 2k_f + k_{s1} - 2(k_f - k_{s1})\phi_1 / \phi_1(k_f - k_{s1}) + k_{s1} + 2k_f$

Table 1. Properties of nanofluid⁴³.

comparison of Nu results at disk and cone with those of previous research utilizing just the common parameters. It analyzed the best agreement between both results published and current work.

Graphical plots

See Figs. 2, 3, 4, 5, 6, 7, 8, 9 and Tables 4, 5, 6.

Properties	Formula
Density (ρ_{hnf})	$\rho_{hnf} = \phi_2 \rho_{s2} + (1 - \phi_2)((1 - \phi_1)\rho_f + \phi_1 \rho_{s1})$
Viscosity (μ_{hnf})	$\mu_{hnf} = \mu_f / (1 - \phi_2)^{2.5} (1 - \phi_1)^{2.5}$
Heat capacity ($(\rho C_p)_{hnf}$)	$(\rho C_p)_{hnf} \left(= \phi_2 (\rho C_p)_{s2} + (1 - \phi_2) \left(\frac{(1 - \phi_1)(\rho C_p)_f}{+ \phi_1 (\rho C_p)_{s1}} \right) \right)$
Thermal conductivity (k_{hnf})	$\frac{k_{hnf}}{k_{nf}} = (k_{s2} + 2k_{hnf} - 2(k_{hnf} - k_{s2})\phi_2 / k_{s2} + 2k_{hnf} + \phi_2(k_{hnf} - k_{s2}))$, Here $\frac{k_{hnf}}{k_{nf}} = (k_{s1} + 2k_f - 2(k_f - k_{s1})\phi_1 / k_{s1} + 2k_f + \phi_1(k_f - k_{s1}))$

Table 2. Properties of hybrid nanofluid⁴³.

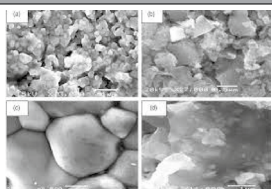


Particles	ρ Density	C_p Heat capacity	k Thermal conductivity
 $COFe_2O_4$	4907	700	3.7
 Ag	10,500	230	418
 H_2O	997.1	4179	0.613

Table 3. Nanoparticle's thermophysical properties^{44,45}.

Final observations

In the current work, real uses of hybrid nano liquid containing $Ag + COFe_2O_4$ nanoparticles and water as a based fluid are measured against velocity and temperature profiles. The main consequences are as follows:

- The velocity distributions profiles are reduced for the superior estimations of the volume segment of nanoparticles ϕ_1 and volume segment of nanoparticles ϕ_2
- The velocity distribution profile is decreased for the higher magnitude of the magnetic parameter M . Here comparative study is investigated and reliable lines for hybrid nanofluid $Ag - COFe_2O_4$ and dashes lines for nanofluid $COFe_2O_4$.

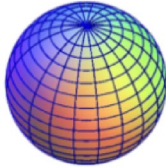
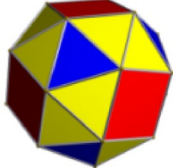

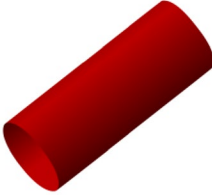
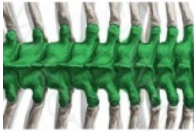
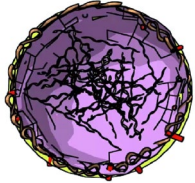
Shape name	Shape factor
<p>Sphere</p> 	3.0
<p>Hexahedron</p> 	3.7
<p>Tetrahedron</p> 	4.0
<p>Cylinders</p> 	4.9
<p>Column</p> 	6.3
<p>Lamina</p> 	16.1

Table 4. Geometrical appearance and shape factor^{46,47}.

- The temperature distributions profile is boosted up for the greater values of the volume segment of nanoparticles ϕ_1
- The temperature distributions profile is boomed for the greater values of volume fraction of nanoparticles ϕ_2

(M)	Moatimid et al. ⁴⁸	Rooman et al. ⁴⁹	Current work
0.0	1.1175	1.1175289	1.1175293
0.1	1.114	1.1103288	1.1103290
0.2	1.1105	1.1021636	1.1021644
0.3	1.107	1.0928879	1.0928889
0.4	1.1035	1.0823038	1.0823037
0.5	1.1	1.0702154	1.0702159

Table 5. Variation of magnetic parameter via Nusselt number^{48,49}.

n	$\theta'(0)$			$\theta'(1)$		
	Turkylmazoglu ⁴¹	Gul et al. ⁴²	Current work	Turkylmazoglu ⁴¹	Gul et al. ⁴²	Current work
1	0.757932	0.758845	0.7590311	1.420219	1.421320	1.422432
2	0.766821	0.767734	0.7681200	1.431320	1.432431	1.433541
3	0.775701	0.776623	0.7770101	1.442431	1.443542	1.444654

Table 6. Comparison of Nusselt number results for disk and cone with those of previous research^{41,42} utilizing just the common parameters.

Data availability

All data generated or analyzed during this study are included in this manuscript.

Received: 12 December 2022; Accepted: 27 March 2023

Published online: 01 April 2023

References

- Choi, S., & Eastman, J. Enhancing thermal conductivity of fluids with nanoparticles. In Proceedings of the ASME International Mechanical Engineering Congress and Exposition, San Francisco, CA, USA, 12–17 November 1995.
- Buongiorno, J. Convective transport in nanofluids. *J. Heat Transfer* **128**, 240–250 (2006).
- Katiyar, A. et al. A general peridynamics model for multiphase transport of non-Newtonian compressible fluids in porous media. *J. Comput. Phys.* **402**, 109075 (2020).
- Khan, M. I., Nigar, M., Hayat, T. & Alsaedi, A. On the numerical simulation of stagnation point flow of non-Newtonian fluid (Carreau fluid) with Cattaneo-Christov heat flux. *Comput. Methods Programs Biomed.* **187**, 105221 (2020).
- Tlili, I., Naseer, S., Ramzan, M., Kadry, S. & Nam, Y. Effects of chemical species and nonlinear thermal radiation with 3D Maxwell nanofluid flow with double stratification—An analytical solution. *Entropy* **22**(4), 453 (2020).
- Na, W., Shah, N. A., Tlili, I. & Siddique, I. Maxwell fluid flow between vertical plates with damped shear and thermal flux: free convection. *Chin. J. Phys.* **65**, 367 (2020).
- Sohail, M. & Naz, R. Modified heat and mass transmission models in the magnetohydrodynamic flow of Sutterby nanofluid in stretching cylinder. *Physica A: Stat. Mech. Appl.* **1**, 1248 (2020).
- Saeed, A. et al. Darcy–Forchheimer MHD hybrid nanofluid flow and heat transfer analysis over a porous stretching cylinder. *Coatings* **10**(4), 391 (2020).
- Babazadeh, H., Zeeshan, A., Jacob, K., Hajizadeh, A. & Bhatti, M. M. Numerical modeling for nanoparticle thermal migration with effects of the shape of particles and magnetic field inside a porous enclosure. *Iran. J. Sci. Technol. Trans. Mech. Eng.* **1**, 1–11 (2020).
- Ullah, N., Nadeem, S. & Khan, A. U. Finite element simulations for the natural convective flow of a nanofluid in a rectangular cavity having corrugated heated rods. *J. Therm. Anal. Calorim.* **1**, 1–13 (2020).
- Li, Y. et al. A numerical exploration of modified second-grade nanofluid with motile microorganisms, thermal radiation, and Wu's slip. *Symmetry* **12**(3), 393 (2020).
- Waqas, H., Farooq, U., Shah, Z., Kumam, P. & Shutaywi, M. Second-order slip effect on bio-convective viscoelastic nanofluid flow through a stretching cylinder with swimming microorganisms and melting phenomenon. *Sci. Rep.* **11**(1), 11208 (2021).
- Rashid, I., Sagheer, M. & Hussain, S. Exact solution of stagnation point flow of MHD Cu–H₂O nanofluid induced by an exponentially stretching sheet with thermal conductivity. *Phys. Scr.* **95**(2), 025207 (2020).
- Xian, H. W., Sidik, N. A. C. & Saidur, R. Impact of different surfactants and ultrasonication time on the stability and thermophysical properties of hybrid nanofluids. *Int. Commun. Heat Mass Transf.* **110**, 104389 (2020).
- Rabbi, K. M. et al. Prediction of MHD flow and entropy generation by Artificial Neural Network in a square cavity with heater-sink for nanomaterial. *Physica A* **541**, 123520 (2020).
- Ghalambaz, M., Doostani, A., Izadpanahi, E. & Chamkha, A. J. Conjugate natural convection flow of Ag–MgO/water hybrid nanofluid in a square cavity. *J. Therm. Anal. Calorim.* **139**(3), 2321–2336 (2020).
- Huminić, G. & Huminić, A. Entropy generation of nanofluid and hybrid nanofluid flow in thermal systems: a review. *J. Mol. Liq.* **302**, 112533 (2020).
- Tayebi, T. & Öztop, H. F. Entropy production during natural convection of hybrid nanofluid in an annular passage between horizontal confocal elliptic cylinders. *Int. J. Mech. Sci.* **171**, 105378 (2020).
- Xian, H. W., Sidik, N. A. C. & Saidur, R. Impact of different surfactants and ultrasonication time on the stability and thermophysical properties of hybrid nanofluids. *Int. Commun. Heat Mass Transfer* **110**, 104389 (2020).
- Awais, M. et al. MHD effects on ciliary-induced peristaltic flow coatings with rheological hybrid nanofluid. *Coatings* **10**(2), 186 (2020).

21. Waini, I., Ishak, A. & Pop, I. MHD flow and heat transfer of a hybrid nanofluid past a permeable stretching/shrinking wedge. *Appl. Math. Mech.* **41**(3), 507–520 (2020).
22. Farooq, U. *et al.* Thermally radioactive bioconvection flow of Carreau nanofluid with modified Cattaneo–Christov expressions and exponential space-based heat source. *Alex. Eng. J.* **60**(3), 3073–3086 (2021).
23. Reddy, P. S., Sreedevi, P. & Reddy, V. N. Entropy generation and heat transfer analysis of magnetic nanofluid flow inside a square cavity filled with carbon nanotubes. *Chem. Thermodyn. Therm. Anal.* **6**, 100045 (2022).
24. Reddy, P. S., Sreedevi, P. & Venkateswarlu, S. Impact of modified Fourier's heat flux on the heat transfer of MgO/Fe₃O₄-Eg-based hybrid nanofluid flow inside a square chamber. *Waves Random Complex Media* **1**, 1–23 (2022).
25. Sreedevi, P. & Reddy, P. S. Entropy generation and heat transfer analysis of alumina and carbon nanotubes based hybrid nanofluid inside a cavity. *Phys. Scr.* **96**(8), 085210 (2021).
26. Sudarsana Reddy, P. & Sreedevi, P. Effect of zero mass flux condition on heat and mass transfer analysis of nanofluid flow inside a cavity with magnetic field. *Eur. Phys. J. Plus* **136**(1), 1–24 (2021).
27. Reddy, P. S., Sreedevi, P. & Chamkha, A. J. Magnetohydrodynamic (MHD) boundary layer heat and mass transfer characteristics of nanofluid over a vertical cone under convective boundary condition. *Propuls. Power Res.* **7**(4), 308–319 (2018).
28. Reddy, P. S., Sreedevi, P. & Chamkha, A. J. Hybrid nanofluid heat and mass transfer characteristics over a stretching/shrinking sheet with slip effects. *J. Nanofluids* **12**(1), 251–260 (2023).
29. Dero, S. *et al.* Thermal stability of hybrid nanofluid with viscous dissipation and suction/injection applications: dual branch framework. *J. Indian Chem. Soc.* **99**(6), 100506 (2022).
30. Haq, F. *et al.* Theoretical investigation of radiative viscous hybrid nanofluid towards a permeable surface of cylinder. *Chin. J. Phys.* **77**, 2761–2772 (2022).
31. Abbasi, A. *et al.* A comparative thermal investigation for modified hybrid nanofluid model (Al₂O₃-SiO₂-TiO₂)/(C₂H₆O₂) due to curved radiated surface. *Case Stud. Therm. Eng.* **37**, 102295 (2022).
32. Hassan, M., El-Zahar, E. R., Khan, S. U., Rahimi-Gorji, M. & Ahmad, A. Boundary layer flow pattern of heat and mass for homogenous shear thinning hybrid-nanofluid: An experimental data base modeling. *Numer. Methods Part. Differ. Equ.* **37**(2), 1234–1249 (2021).
33. Madhukesh, J. K. *et al.* Numerical simulation of AA7072-AA7075/water-based hybrid nanofluid flow over a curved stretching sheet with Newtonian heating: A non-Fourier heat flux model approach. *J. Mol. Liquids* **335**, 116103 (2021).
34. Reddy, P. S. & Sreedevi, P. Effect of thermal radiation on heat transfer and entropy generation analysis of MHD hybrid nanofluid inside a square cavity. *Waves Random and Complex Med.* **1**, 1–33 (2022).
35. Khan, W. Multiple Exact Solutions of Second Degree Nanofluid Slip Flow and Heat Transport in Porous Medium. Available at SSRN 4231915.
36. Farooq, U. *et al.* Modeling and computational framework of radiative hybrid nanofluid configured by a stretching surface subject to entropy generation: Using Keller box scheme. *Arab. J. Chem.* **16**(4), 1028 (2023).
37. Farooq, U. *et al.* Numerical treatment of casson nanofluid bioconvective flow with heat transfer due to stretching cylinder/plate: Variable physical properties. *Arab. J. Chem.* **1**, 104589 (2023).
38. Yaseen, M., Rawat, S. K., Shah, N. A., Kumar, M. & Eldin, S. M. Ternary hybrid nanofluid flow containing gyrotactic microorganisms over three different geometries with Cattaneo–Christov model. *Mathematics* **11**(5), 1237 (2023).
39. Farooq, U. *et al.* Computation of Cattaneo–Christov heat and mass flux model in Williamson nanofluid flow with bioconvection and thermal radiation through a vertical slender cylinder. *Case Stud. Therm. Eng.* **1**, 102736 (2023).
40. Usafzai, W. K. Multiple exact solutions of second degree nanofluid slip flow and heat transport in porous medium. *Therm. Sci. Eng. Progr.* **1**, 101759 (2023).
41. Turkiymazoglu, M. On the fluid flow and heat transfer between a cone and a disk both stationary or rotating. *Math. Comput. Simul.* **177**, 329–340 (2020).
42. Gul, T. *et al.* CNTs-nanofluid flow in a rotating system between the gap of a disk and cone. *Phys. Scr.* **95**(12), 125202 (2020).
43. Devi, S. U. & Devi, S. A. Heat transfer enhancement of Cu–Al₂O₃/water hybrid nanofluid flow over a stretching sheet. *J. Niger. Math. Soc.* **36**(2), 419–433 (2017).
44. Gul, T., Bilal, M., Alghamdi, W., Asjad, M. I. & Abdeljawad, T. Hybrid nanofluid flow within the conical gap between the cone and the surface of a rotating disk. *Sci. Rep.* **11**(1), 1–19 (2021).
45. Acharya, N., Maity, S. & Kundu, P. K. Framing the hydrothermal features of magnetized TiO₂-CoFe₂O₄ water-based steady hybrid nanofluid flow over a radiative revolving disk. *Multidiscip. Model. Mater. Struct.* **1**, 1 (2019).
46. Ghadikolaei, S. S., Yassari, M., Sadeghi, H., Hosseinzadeh, K. & Ganji, D. D. Investigation on thermophysical properties of TiO₂-Cu/H₂O hybrid nanofluid transport dependent on shape factor in MHD stagnation point flow. *Powder Technol.* **322**, 428–438 (2017).
47. Dinarvand, S. & Rostami, M. N. Three-dimensional squeezed flow of aqueous magnetite-graphene oxide hybrid nanofluid: A novel hybridity model with analysis of shape factor effects. *Proc. Inst. Mech. Eng. Part E: J. Process. Mech. Eng.* **234**(2), 193–205 (2020).
48. Moatimid, G. M., Mohamed, M. A. & Elagamy, K. A Casson nanofluid flow within the conical gap between rotating surfaces of a cone and a horizontal disc. *Sci. Rep.* **12**(1), 11275 (2022).
49. Rooman, M. *et al.* Statistical modeling for Ree-Eyring nanofluid flow in a conical gap between porous rotating surfaces with entropy generation and Hall Effect. *Sci. Rep.* **12**(1), 21126 (2022).

Acknowledgements

“This study is supported over funding from Prince Sattam bin Abdulaziz University project number (PSAU/2023/R/1444)”.

Author contributions

U.F. modeled and solved the problem. M.I. and H. W. verified and proof read the manuscript. S.N. and U.F. has contributed in the numerical computations and plotting the graphical results. N.F. and A.M.G. has improved the language structure of revised manuscript and simulated the results for accuracy purpose. A.A. and A.B. reviewed the revised manuscript and technically correction was made. All authors are agreed on the final draft of the submission file.

Competing interests

The authors declare no competing interests.

Additional information

Correspondence and requests for materials should be addressed to A.B.

Reprints and permissions information is available at www.nature.com/reprints.

Publisher's note Springer Nature remains neutral with regard to jurisdictional claims in published maps and institutional affiliations.



Open Access This article is licensed under a Creative Commons Attribution 4.0 International License, which permits use, sharing, adaptation, distribution and reproduction in any medium or format, as long as you give appropriate credit to the original author(s) and the source, provide a link to the Creative Commons licence, and indicate if changes were made. The images or other third party material in this article are included in the article's Creative Commons licence, unless indicated otherwise in a credit line to the material. If material is not included in the article's Creative Commons licence and your intended use is not permitted by statutory regulation or exceeds the permitted use, you will need to obtain permission directly from the copyright holder. To view a copy of this licence, visit <http://creativecommons.org/licenses/by/4.0/>.

© The Author(s) 2023